Primordial Helium Abundance: A Reanalysis of the Izotov-Thuan Spectroscopic Sample

Masataka Fukugita[(a,b)] and Masahiro Kawasaki[(a)]

[(a)] *Institute for for Cosmic Ray Research, University of Tokyo, Kashiwa 277-8582, Japan*

[(b)] *Institute for Advanced Study, Princeton, NJ 08540 USA*

Abstract

A reanalysis is made for the helium abundance determination for the Izotov-Thuan (2004) spectroscopic sample of extragalactic H II regions. We find that the effect of underlying stellar absorption of the He I lines, which is more important for metal poor systems, affects significantly the inferred primordial helium abundance Y_p obtained in the zero metallicity limit and the slope of linear extrapolation, dY/dZ. This brings Y_p from 0.234 ± 0.004 to 0.250 ± 0.004 and $dY/dZ = 4.7\pm1.0$ to 1.1 ± 1.4. Conservatively, this indicates the importance of the proper understanding of underlying stellar absorption for accurate determinations of the primordial helium abundance to the error of $\delta Y_p \simeq 0.002 - 0.004$.

1. Introduction

Izotov and Thuan (2004; hereinafter IT04) presented the primordial helium abundance $Y_p = 0.242 \pm 0.002$, consistently with their earlier publications (Izotov and Thuan 1998, and references therein), from helium recombination lines in metal poor extragalactic HII regions. This is significantly higher than the earlier values given by a number of authors (Pagel et al. 1992; Olive et al. 1997; Peimbert et al. 2000), yet is significantly lower by three standard deviations than the expectation from the baryon abundance constrained from CMB temperature anisotropies (Spergel et al. 2003) with the aid of Big-Bang nucleosynthesis [1]. Particularly intriguing is the small errors which are common to nearly all analyses. We suspect that this might not represent properly the error including systematics.

IT04 provided high quality spectroscopic data for 33 HII regions detailed enough for us to repeat the analysis. In this paper we are particularly concerned with the effect induced by

[1] We adopt here the neutron lifetime from the conventional decay counting of ultra cold neutrons (Eidelman et al. 2004).

underlying stellar absorption on nebula helium emission lines that is poorly constrained. Our analysis is along the line of Peimbert et al. (2002) and Olive and Skillman (2004; hereinafter OS04), who introduced the helium absorption strength as a free parameter, although ours are somewhat more conservative. OS04 and Peimbert et al. (2000; 2002) presented an analysis in which plasma temperature is also determined by the helium emission lines alone. However, this, in principle proper approach given accurate data, induces large errors in the resulting helium abundance with the present accuracy of the available data for distant HII regions, and a trend that might be brought about with the inclusion of stellar absorption is buried in the noise. Since we do not see a compelling reason that plasma temperatures from helium and oxygen are significantly different, we take the approach that plasma temperature is determined by the ratio of oxygen emission lines, as was done in most of the work including IT04, and study the effect of stellar absorption by introducing it as a free parameter. We show that Y_p and dY/dZ are very sensitive to the introduction of the underlying stellar absorption of the helium lines.

2. Data and procedures of the analysis

We consider 30 of the 33 H II regions given in IT04,[2] discarding 3 H II regions (UM133, Mrk1063, HS0111+2115), for which He I λ4026 line is not detected. We also add NGC346 (Region A) studied by Peimbert et al. (2000). The 31 H II regions we studied are shown in Table 1, where our final results are also presented. The plasma temperature of OIII is determined from the ratio of [O III] emissions λ4363 versus $\lambda\lambda$4959,5007. The extinction and stellar absorption of H I Balmer lines are derived from Hα, Hβ, Hγ and Hδ using the recombination calculation of Hummer & Storey (1987) for the intrinsic line intensity ratios $I(\lambda)/I(\mathrm{H}\beta)$, as

$$\frac{I(\mathrm{H}\lambda)}{I(\mathrm{H}\beta)} = \frac{F(\lambda)}{F(\mathrm{H}\beta)} \frac{W(\mathrm{H}\lambda) + a_{\mathrm{HI}}}{W(\mathrm{H}\beta) + a_{\mathrm{HI}}} \frac{W(\mathrm{H}\beta)}{W(\mathrm{H}\lambda)} 10^{f(\lambda)c_{\mathrm{H}\beta}}. \quad (1)$$

where $F(\lambda)$ is the observed line intensity, $W(\lambda)$ is the equivalent width, a_{HI} is the stellar absorption and $f(\lambda)c_{\mathrm{H}\beta}$ is the extinction relative to Hβ. The inclusion of H9 and higher Balmer lines, where available, does not modify the result beyond our interest. H8 is blended with He Iλ3889, and equation (1) is used to deblend the helium line. We discard H7 that is deblended with [Ne III]. We use the extinction curve of O'Donnel (1994), but the use of the different extinction curve leads only to a small difference that can be ignored here.

[2]We do not include the sample of Izotov & Thuan (1998) because the equivalent widths are not provided for the recombination lines.

We consider six He I lines, five lines for orthohelium λ3890 ($3s \rightarrow 2p$), λ4026 ($5d \rightarrow 2p$), λ4471 ($4d \rightarrow 2p$), λ5875 ($3d \rightarrow 2p$), λ7065 ($3s \rightarrow 2p$), and one line for parahelium λ6678 ($3d \rightarrow 2p$). The λ3890 and λ7065 are sensitive to a fluorescent correction and thus to the radiative transfer. λ4026 is generally weak, susceptible largely to stellar absorption. We use the effective recombination coefficients of Benjamin et al. (1999), which include collisional excitation, and the radiative transfer calculation of Benjamin et al. (2002) for fluorescent corrections, f_λ, which is controlled by the optical depth $\tau(3890)$. We calculate the abundance of singly ionised helium as

$$y^+ = \frac{F(\mathrm{HeI}\lambda)}{F(\mathrm{H}\beta)} \frac{I(\mathrm{H}\beta)}{I(\mathrm{HeI}\lambda)} \frac{W(\mathrm{H}\beta)}{W(\mathrm{H}\beta)+a_{\mathrm{HI}}} \frac{W(\mathrm{HeI}\lambda)+a_{\mathrm{HeI}}}{W(\mathrm{HeI}\lambda)} 10^{f(\lambda)c_{\mathrm{H}\beta}} \frac{1}{f_\lambda}. \quad (2)$$

This is the same as that adopted by OS04 and that by IT04 up to the inclusion of a_{HeI}. We do not know what ratios are to be taken for a_{HeI} for different lines. We assume here that all absorption strengths are identical in equivalent strengths, as was done in OS04. This is probably not too bad an approximation in view of the observation for absorption in B stars (Lennon et al. 1993; Lyubimkov et al. 2000) and the size of the resulting errors in our calculation that amount to $\approx$50% of the central values: more detailed line ratios are the matter at a higher order level. We refer to Olive & Skillman (2001) for more detailed discussion for this issue.

Our method of analysis differs from the usual one to find the parameters. We find the best likelihood solution in full four parameter space y^+, n_e (electron density), a_{HeI} and τ for six lines, rather than minimising the sum of χ^2 for each line, which has been adopted in the literature, for the purpose to take the correlation among the lines into account. The electron density is poorly constrained, but its indeterminacy affects the resulting Y little due to its very weak dependence in the recombination coefficient.

We add the abundance of doubly ionised helium y^{++} to calculate Y when He II λ4686 is detected. We take the oxygen abundance from IT04. The final results are displayed for the mass fraction of helium Y as a function of the oxygen abundance relative to hydrogen O/H, and linear extrapolation is employed to obtain the primordial helium abundance Y_p in the zero oxygen abundance limit (Peimbert & Torres-Peimbert 1974),

$$Y = Y_p + \frac{dY}{d(\mathrm{O/H})} \left(\frac{\mathrm{O}}{\mathrm{H}} \right). \quad (3)$$

We adopt $dY/d(\mathrm{O/H}) = 18.2 dY/dZ$ from IT04.

3. Results

Extinction and stellar absorption of the hydrogen lines are determined from the 4 Balmer lines. The extinction parameter $c_{\rm H\beta}$ agrees very well with those of IT04 in spite of the different extinction curves used. Curiously, the stellar absorption we derived is generally somewhat larger than that of IT04, although we do not claim that the two are inconsistent since errors are generally large. For most of the case absorption strengths lie in the range of $0-6$Å, but for two it is larger than 10Å. The mean is $a_{\rm HI} = 2.5\pm3.5$Å, where the error stands for the standard deviation. This is a natural value for HII regions. As noted by OS04, we find negative values for absorptions for 11 HII regions. This occurrence is expected from a large scatter in $a_{\rm HI}$, but might be ascribed to the collisional excitation for hydrogen emission lines that are not taken into account. In any case, the error induced by resetting the negative absorption width to zero will be small for the helium emissivity analysis, since the reference Hβ has a large equivalent width > 200Å.

To confirm that our results agree with those of IT04 when He I stellar absorption is ignored, we first carry out the analysis assuming $a_{\rm HeI} = 0$. The helium abundance plotted as a function of the oxygen abundance [O/H] presented in Figure 1(a) confirms the trend seen in IT04, although individual data scatter more with our analysis. We obtain $Y_p = 0.234\pm0.003$ consistent with 0.2385 ± 0.0015 from the extrapolation of the results tabulated in IT04 [see Figure 2(a)][3] Our χ^2 is rather poor: the mean is $\overline{\chi^2} = 5.9$. There are five cases (HS 0122+0743, Mrk724, POX36, HS0128+2832 and Mrk 1236) that give $\chi^2 > 10$, implying the inadequacy of the procedure we assumed.

When we include $a_{\rm HeI}$ as a free parameter, and carry out a similar analysis, χ^2 is enormously improved: we find $\overline{\chi^2} = 2.0$, which is dominated by a few bad fits, notably by one system giving $\chi^2 = 6.1$ with the zero He I absorption width. For all cases, except one, that showed poor χ^2 with $a_{\rm HeI} = 0$, fits are greatly improved. In particular for the five cases of poor fit we noted above χ^2 drops from 29.5 to 1.2 for HS0122+0743, 10.1 to 2.5 for Mrk724, 10.1 to 1.0 for POX36. and 18.5 to 0.9 for HS0128+2832, and from 10.6 to 4.4 for Mrk 1236, indicating the need to take the stellar absorption into account.

Figure 1(b) shows the plot that can be compared with Figure 1(a) but with a non-vanishing $a_{\rm HeI}$. It is interesting to see that the derived helium abundance is more strongly affected for metal poor HII regions, pushing up the helium abundance extrapolated to the zero metallicity quite a bit and resulting in $Y_p = 0.250 \pm 0.004$. Note that the large scatter

[3]IT04 give Y for individual HII regions but do not give Y_p for their new data alone. They combined with their 1998 data and present $Y_p = 0.2429 \pm 0.0009$.

around the extrapolation line seen in panel (a) is not visible in this plot any more. The χ^2 curves are given in Figure 2(a) for Y_p and for $dY/d(\mathrm{O/H})$ (b) which is discussed below.

The absorption widths derived from our fit have generally large errors, $\approx 50\%$. The mean absorption equivalent widths are $a_{\mathrm{HeI}} = 0.40 \pm 0.31$. There are 6 HII regions for which the central values of a_{HeI} are negative. The four among six are the cases for which the fits without stellar absorption gave unusually good χ^2. The only cases that are marginally acceptable are with HS1028+3843 ($\chi^2 = 3.6$) and Mrk35 ($\chi^2 = 6.1$). (In the analysis with $a_{\mathrm{HeI}} = 0$, 10 systems have χ^2 greater than 6.1.)

OS04 presented their analysis for seven HII regions common in our sample. A comparison shows that our Y is always consistent with theirs within one standard deviation, although the errors are significantly larger in OS04 due to larger uncertainties in the temperature of the plasma. We find other parameters, such as temperature, are also consistent.

Figure 3 shows the average absorption equivalent width that varies with the heavy element abundance. Although individual data show a rather large scatter, the trend is clear in this binned plot: the stellar absorption effect is more important for metal poor HII regions[4]. Since the oxygen abundance shows a tight anticorrelation with temperature of the plasma, this figure is also interpreted as showing the correlation of the stellar absorption with the plasma temperature: Higher the temperature, more the important absorption. This is the systematic trend that largely modifies the extrapolation of the helium abundance to the zero metallicity.

In this connection another interesting quantity is $dY/d(\mathrm{O/H})$, i.e., the increment of helium per heavy element production. The IT04 results give $dY/d(\mathrm{O/H}) = 82 \pm 15$ (or $dY/dZ = 4.5 \pm 0.8$, which is consistent with the final result IT04 quoted, $dY/dZ = 3.7 \pm 1.2$) from a sample of seven HII regions. Our analysis with a_{HeI} set equal to zero gives $dY/d(\mathrm{O/H}) = 86 \pm 18$ or $dY/dZ = 4.7 \pm 1.0$. On the other hand, with stellar absorption we obtain $dY/d(\mathrm{O/H}) = 20 \pm 25$ or $dY/dZ = 1.1 \pm 1.4$, which is a drastic decrease.

We remark that IT04 use only 3 lines in deriving the helium abundance, dropping λ3889, λ4026 and λ7065, with the anticipation that the other 3 bright lines are less affected by stellar absorption, while they use λ3889 and λ7065 to constrain other parameters. We also tried to drop the three lines when we calculate Y, but the results remain unchanged from the full 6 line analysis.

[4]While our derived parameters are consistent with those of OS04, the effect is not discernible in OS04 due to larger errors (introduced by the temperature uncertainty) and their smaller data set.

4. Conclusions

Using the IT04 sample we showed that the neglect of the stellar absorption on the helium emission lines causes a large systematic effect on Y_p and dY/dZ. This is due to the fact that the stellar absorption equivalent width shows a trend that increases towards metal poor systems. The inclusion of helium stellar absorption improves enormously the acceptance of fit to the He I emission data, especially when the quality was bad without the inclusion of stellar absorption. The resulting magnitude of the absorption equivalent width of He I λ4471 line (and also of the H I Balmer lines) is on the order that is expected in a population synthesis calculation (González Delgado et al. 1999) for the nebula phase.

With the inclusion of stellar absorption we obtained the primordial helium abundance increased from $y_p = 0.234 \pm 0.004$ to 0.250 ± 0.004. We do not claim that the latter is the true value, but it is much preferred to the former on the ground of much smaller χ^2 for the fit to individual HII regions, while the 6-line fit without stellar absorption is barely acceptable. Or, most conservatively, one can claim that we cannot obtain the primordial helium abundance to the error of $\delta Y_p \approx 0.004$ or less unless underlying stellar absorption is properly understood.

In our analysis we noted that the minimisation of the sum of the χ^2 over individual lines, ignoring the correlation among lines, is likely to underestimate the error.

If we accept our higher helium abundance, we find $n_B/n_\gamma = 7.9^{+4.0}_{-2.4} \times 10^{-10}$ with the aid of the standard Big Bang nucleosynthesis calculation (e.g., Olive et al. 2001). This baryon abundance is consistent with that inferred from cosmic microwave background anisotropies (Spergel et al. 2003).

We also found that dY/dZ is largely affected upon the inclusion of stellar absorption: the original value of $dY/dZ \approx 4 - 5$ decreases to 1 ± 1. This smaller number is consistent with the derivative inferred form the standard solar model (Bahcall et al. 2001) $\Delta Y/\Delta Z = (Y_{\rm initial} - Y_p)/Z_{\rm initial} = 1.4$, and also with 2.1 ± 0.4 from the dwarf star atmosphere (Jimenez et al. 2003) using the method introduced by Pagel and Portinari (1998) who presented 3 ± 2 for this derivative.

This work is supported in part by Grants in Aid of the Ministry of Education of Japan at Kashiwa. MF received support from the Monell Foundation at Princeton.

REFERENCES

Bahcall, J. N., Pinsonneault, M. H., & Basu, S. 2001, ApJ, 555, 990

Benjamin, R. A., Skillman, E. D., & Smits, D. P. 1999, ApJ, 514, 307

Benjamin, R. A., Skillman, E. D., & Smits, D. P. 2002, ApJ, 569, 288

Eidelman, S. et al. (Particle data Group) 2004, Phys. Lett. B592, 1

González Delgado, R. M., Leitherer, C., & Heckman, T. M. 1999, ApJS, 125, 489

Hummer, D. G., & Storey, P. J. 1987, MNRAS, 224, 801

Izotov, Y. I., & Thuan, T. X. 1998, ApJ, 500, 188

Izotov, Y. I., & Thuan, T. X. 2004, ApJ, 602, 20 (IT04)

Jimenez, R., Flynn, C., MacDonald, J., & Gibson, B. K. 2003, Science, 299, 1552

Lennon, D. J., Dufton, P. L., & Fitzsimmons, A. 1993, A&AS, 97, 559

Lyubimkov, L. S., Lambert, D. L., Rachkovskaya, T. M., Rostopchin, S. I., Tarasov, A. E., Poklad, D. B., Larionov, V. M., & Larionova, L. V. 2000, MNRAS, 316, 19

O'Donnell, J. E. 1994, ApJ, 422, 158

Olive, K. A., & Skillman, E. D. 2001, New Astronomy, 6, 119

Olive, K. A., & Skillman, E. D. 2004, ApJ, 617, 29 (OS04)

Olive, K. A., Skillman, E. D. 2004,& Steigman, G., 1997, ApJ, 483, 788

Olive, K. A., Steigman, G., & Walker, T. P. 2000, Phys. Rep., 333, 389

Pagel, B. E. J., & Portinari, L. 1998, MNRAS, 298, 747

Pagel, B. E. J., Simonson, E. A., Terlevich, R. J., & Edmunds, M. G. 1992, MNRAS, 255, 325

Peimbert, M., & Torres-Peimbert, S. 1974, ApJ, 193, 327

Peimbert, M., Peimbert, A., & Ruiz, M. T. 2000, ApJ, 541, 688

Peimbert, A., Peimbert, M., & Luridiana, V. 2002, ApJ, 565, 668

Spergel, D. N., et al. 2003, ApJS, 148, 175

Table 1. Physical Properties of HII Regions and Helium Abundance

HII reion	O/H [$\times 10^{-4}$]	$T_e[10^4 K]$	C_{H_β}	a(HI) [Å]	n_e [cm^{-3}]	τ	a(HeI) [Å]	Y	χ^2	Y (w/o abs)	χ^2 (w/o abs)
J 0519+0007	0.270 ± 0.009	2.073 ± 0.034	0.254 ± 0.020	0.00 ± 0.27	210^{+159}_{-139}	$3.76^{+0.75}_{-0.78}$	$0.49^{+0.41}_{-0.34}$	$0.2586^{+0.0134}_{-0.0145}$	0.77	$0.2448^{+0.0115}_{-0.0111}$	2.98
HS 2236+1344	0.296 ± 0.008	2.122 ± 0.029	0.134 ± 0.024	4.98 ± 1.31	170^{+157}_{-142}	$4.56^{+1.06}_{-0.99}$	$0.17^{+0.46}_{-0.17}$	$0.2458^{+0.0139}_{-0.0132}$	2.99	$0.2410^{+0.0093}_{-0.0091}$	3.13
HS 0122+0743	0.397 ± 0.011	1.786 ± 0.022	0.121 ± 0.024	3.75 ± 1.19	0^{+123}	$0.92^{+0.41}_{-0.78}$	$1.20^{+0.35}_{-0.29}$	$0.2612^{+0.0049}_{-0.0091}$	1.21	$0.2277^{+0.0067}_{-0.0071}$	29.5
HS 0837+4717	0.398 ± 0.010	1.952 ± 0.023	0.246 ± 0.019	0.00 ± 0.09	305^{+88}_{-101}	$6.04^{+0.52}_{-0.53}$	$0.00^{+0.24}$	$0.2541^{+0.0088}_{-0.0064}$	0.88	$0.2541^{+0.0068}_{-0.0064}$	0.88
CGCG007-025(2)	0.547 ± 0.017	1.665 ± 0.026	0.202 ± 0.019	0.00 ± 0.21	0^{+43}	$1.36^{+0.49}_{-0.45}$	$0.47^{+0.39}_{-0.32}$	$0.2508^{+0.0056}_{-0.0055}$	4.73	$0.2448^{+0.0035}_{-0.0041}$	7.09
CGCG007-025(1)	0.596 ± 0.014	1.651 ± 0.017	0.278 ± 0.018	0.00 ± 0.10	115^{+116}_{-102}	$1.44^{+0.50}_{-0.50}$	$0.40^{+0.24}_{-0.22}$	$0.2568^{+0.0071}_{-0.0075}$	2.93	$0.2466^{+0.0051}_{-0.0054}$	6.38
HS 0134+3415	0.720 ± 0.019	1.643 ± 0.017	0.079 ± 0.018	0.00 ± 0.24	0^{+163}	$1.92^{+0.39}_{-0.72}$	$0.42^{+0.40}_{-0.36}$	$0.2566^{+0.0049}_{-0.0111}$	0.05	$0.2478^{+0.0068}_{-0.0091}$	1.44
HS 1028+3843	0.781 ± 0.020	1.593 ± 0.016	0.009 ± 0.023	2.07 ± 1.83	465^{+158}_{-161}	$5.48^{+1.01}_{-0.94}$	$0.0^{+0.16}$	$0.2571^{+0.0072}_{-0.0072}$	3.60	$0.2573^{+0.0070}_{-0.0074}$	3.60
HS 0811+4913	0.928 ± 0.024	1.451 ± 0.015	0.116 ± 0.024	6.21 ± 1.80	195^{+234}_{-195}	$0.32^{+1.05}_{-0.32}$	$0.67^{+0.55}_{-0.48}$	$0.2437^{+0.0114}_{-0.0113}$	1.03	$0.2325^{+0.0066}_{-0.0077}$	3.22
HS 1214+3801	1.044 ± 0.024	1.344 ± 0.012	0.329 ± 0.024	4.59 ± 1.16	285^{+110}_{-206}	$0.00^{+0.71}$	$0.45^{+0.23}_{-0.19}$	$0.2463^{+0.0073}_{-0.0054}$	2.67	$0.2374^{+0.0041}_{-0.0050}$	9.04
Mrk 724	1.076 ± 0.029	1.298 ± 0.014	0.122 ± 0.018	0.00 ± 0.12	80^{+152}_{-80}	$0.20^{+0.58}_{-0.20}$	$0.19^{+0.09}_{-0.08}$	$0.2524^{+0.0056}_{-0.0062}$	2.46	$0.2429^{+0.0040}_{-0.0044}$	10.1
HS 0029+1748	1.101 ± 0.035	1.289 ± 0.015	0.385 ± 0.026	5.11 ± 1.01	0^{+174}	$1.60^{+0.48}_{-0.71}$	$0.27^{+0.27}_{-0.22}$	$0.2468^{+0.0057}_{-0.0064}$	2.58	$0.2420^{+0.0034}_{-0.0075}$	4.11
Mrk 67	1.116 ± 0.046	1.320 ± 0.023	0.190 ± 0.026	1.99 ± 0.58	135^{+628}_{-135}	$1.76^{+1.08}_{-1.42}$	$0.35^{+0.23}_{-0.22}$	$0.2607^{+0.0116}_{-0.0223}$	0.40	$0.2270^{+0.0147}_{-0.0039}$	2.84
POX 36	1.131 ± 0.056	1.256 ± 0.029	0.150 ± 0.019	0.00 ± 0.08	5^{+147}_{-5}	$0.00^{+0.46}$	$0.40^{+0.18}_{-0.16}$	$0.2551^{+0.0054}_{-0.0065}$	0.95	$0.2452^{+0.0034}_{-0.0055}$	10.1
UM 439	1.167 ± 0.029	1.415 ± 0.013	0.234 ± 0.024	1.45 ± 0.78	205^{+232}_{-205}	$3.52^{+0.96}_{-0.91}$	$0.00^{+0.11}$	$0.2446^{+0.0080}_{-0.0079}$	0.92	$0.2447^{+0.0077}_{-0.0080}$	0.92
HS 0924+3821	1.178 ± 0.045	1.261 ± 0.020	0.159 ± 0.025	2.59 ± 0.66	0^{+306}	$0.88^{+0.78}_{-0.88}$	$0.50^{+0.24}_{-0.20}$	$0.2557^{+0.0060}_{-0.0095}$	0.38	$0.2222^{+0.0146}_{-0.0035}$	7.12
Mrk 450 (2)	1.195 ± 0.064	1.247 ± 0.028	0.058 ± 0.027	4.16 ± 1.20	$675^{+\cdots}_{-562}$	$0.32^{+1.25}_{-0.32}$	$0.49^{+0.65}_{-0.49}$	$0.2436^{+0.0178}_{-0.0156}$	2.21	$0.2308^{+0.0154}_{-0.0054}$	3.00
UM 422	1.291 ± 0.036	1.300 ± 0.013	0.119 ± 0.021	0.00 ± 0.97	95^{+293}_{-95}	$0.56^{+0.73}_{-0.56}$	$0.58^{+0.38}_{-0.35}$	$0.2581^{+0.0076}_{-0.0107}$	2.08	$0.2458^{+0.0068}_{-0.0064}$	5.08
HS 0128+2832	1.370 ± 0.033	1.261 ± 0.010	0.408 ± 0.028	11.6 ± 1.8	285^{+386}_{-285}	$2.72^{+1.29}_{-1.14}$	$1.10^{+0.38}_{-0.32}$	$0.2561^{+0.0107}_{-0.0108}$	0.93	$0.2271^{+0.0031}_{-0.0027}$	18.5
Mrk 1236	1.403 ± 0.036	1.229 ± 0.012	0.356 ± 0.024	0.04 ± 1.13	0^{+103}	$2.00^{+0.31}_{-0.45}$	$0.67^{+0.33}_{-0.29}$	$0.2588^{+0.0048}_{-0.0045}$	4.36	$0.2500^{+0.0029}_{-0.0053}$	10.6
NGC 346 (A)	1.416 ± 0.208	1.313 ± 0.009	0.163 ± 0.009	0.87 ± 0.48	0^{+52}	$0.16^{+0.09}_{-0.16}$	$0.15^{+0.13}_{-0.11}$	$0.2485^{+0.0021}_{-0.0026}$	2.33	$0.2462^{+0.0013}_{-0.0018}$	4.04
Mrk 450 (1)	1.422 ± 0.039	1.170 ± 0.012	0.144 ± 0.023	2.96 ± 1.12	170^{+378}_{-170}	$2.96^{+0.90}_{-1.16}$	$0.60^{+0.30}_{-0.26}$	$0.2537^{+0.0066}_{-0.0075}$	1.79	$0.2398^{+0.0062}_{-0.0065}$	7.61
UM 238	1.462 ± 0.049	1.250 ± 0.015	0.235 ± 0.030	15.5 ± 2.9	$700^{+\cdots}_{-481}$	$2.60^{+1.69}_{-0.97}$	$0.98^{+0.71}_{-0.65}$	$0.2473^{+0.0145}_{-0.0131}$	1.29	$0.2324^{+0.0064}_{-0.0039}$	4.03
HS 0735+3512	1.493 ± 0.043	1.206 ± 0.014	0.236 ± 0.023	0.16 ± 0.61	180^{+447}_{-180}	$2.44^{+1.02}_{-1.20}$	$0.25^{+0.22}_{-0.20}$	$0.2576^{+0.0083}_{-0.0108}$	1.44	$0.2489^{+0.0079}_{-0.0099}$	2.98
HS 2359+1659	1.524 ± 0.056	1.192 ± 0.016	0.324 ± 0.025	1.33 ± 1.16	145^{+497}_{-145}	$1.56^{+0.99}_{-1.21}$	$0.00^{+0.25}$	$0.2470^{+0.0065}_{-0.0091}$	0.74	$0.2470^{+0.0060}_{-0.0091}$	0.74
HS 1311+3628	1.525 ± 0.045	1.141 ± 0.013	0.066 ± 0.024	1.48 ± 1.30	$450^{+\cdots}_{-450}$	$0.56^{+1.30}_{-0.56}$	$0.63^{+0.46}_{-0.44}$	$0.2527^{+0.0085}_{-0.0114}$	1.58	$0.2401^{+0.0064}_{-0.0028}$	3.78
HS 1213+3636	1.561 ± 0.087	1.077 ± 0.027	0.019 ± 0.019	0.00 ± 0.61	50^{+193}_{-50}	$0.00^{+0.44}$	$0.48^{+0.36}_{-0.32}$	$0.2597^{+0.0056}_{-0.0057}$	3.50	$0.2533^{+0.0030}_{-0.0038}$	5.91

Table 1—Continued

HII reion	O/H [$\times 10^{-4}$]	$T_e[10^4 K]$	C_{H_β}	a(HI) [Å]	n_e [cm^{-3}]	τ	a(HeI) [Å]	Y	χ^2	Y (w/o abs)	χ^2 (w/o abs)
UM 396	1.708 ± 0.064	1.140 ± 0.015	0.258 ± 0.028	6.31 ± 1.22	$620\ ^{+\cdots}_{620}$	$1.20\ ^{+1.71}_{-0.75}$	$0.00\ ^{+0.21}$	$0.2471\ ^{+0.0094}_{-0.0078}$	1.51	$0.2471\ ^{+0.0081}_{-0.0078}$	1.52
Mrk 1315	1.774 ± 0.041	1.101 ± 0.008	0.149 ± 0.017	0.00 ± 0.31	$310\ ^{+249}_{-231}$	$0.32\ ^{+0.66}_{-0.32}$	$0.15\ ^{+0.24}_{-0.15}$	$0.2554\ ^{+0.0041}_{-0.0043}$	2.85	$0.2533\ ^{+0.0031}_{-0.0030}$	3.34
Mrk 1329	1.787 ± 0.044	1.079 ± 0.009	0.178 ± 0.023	0.82 ± 0.97	$500\ ^{+\cdots}_{-460}$	$0.48\ ^{+1.24}_{-0.48}$	$0.31\ ^{+0.22}_{-0.23}$	$0.2574\ ^{+0.0055}_{-0.0073}$	1.71	$0.2497\ ^{+0.0029}_{-0.0023}$	3.90
Mrk 35	1.977 ± 0.058	1.016 ± 0.012	0.230 ± 0.018	0.00 ± 0.07	$335\ ^{+270}_{-237}$	$2.24\ ^{+0.72}_{-0.71}$	$0.00\ ^{+0.08}$	$0.2554\ ^{+0.0027}_{-0.0023}$	6.10	$0.2555\ ^{+0.0021}_{-0.0024}$	6.10

Note. — The dots in upward errors of n_e means that one sigma value is not reached within the limit ($n_e = 1000$) of our fit we set.

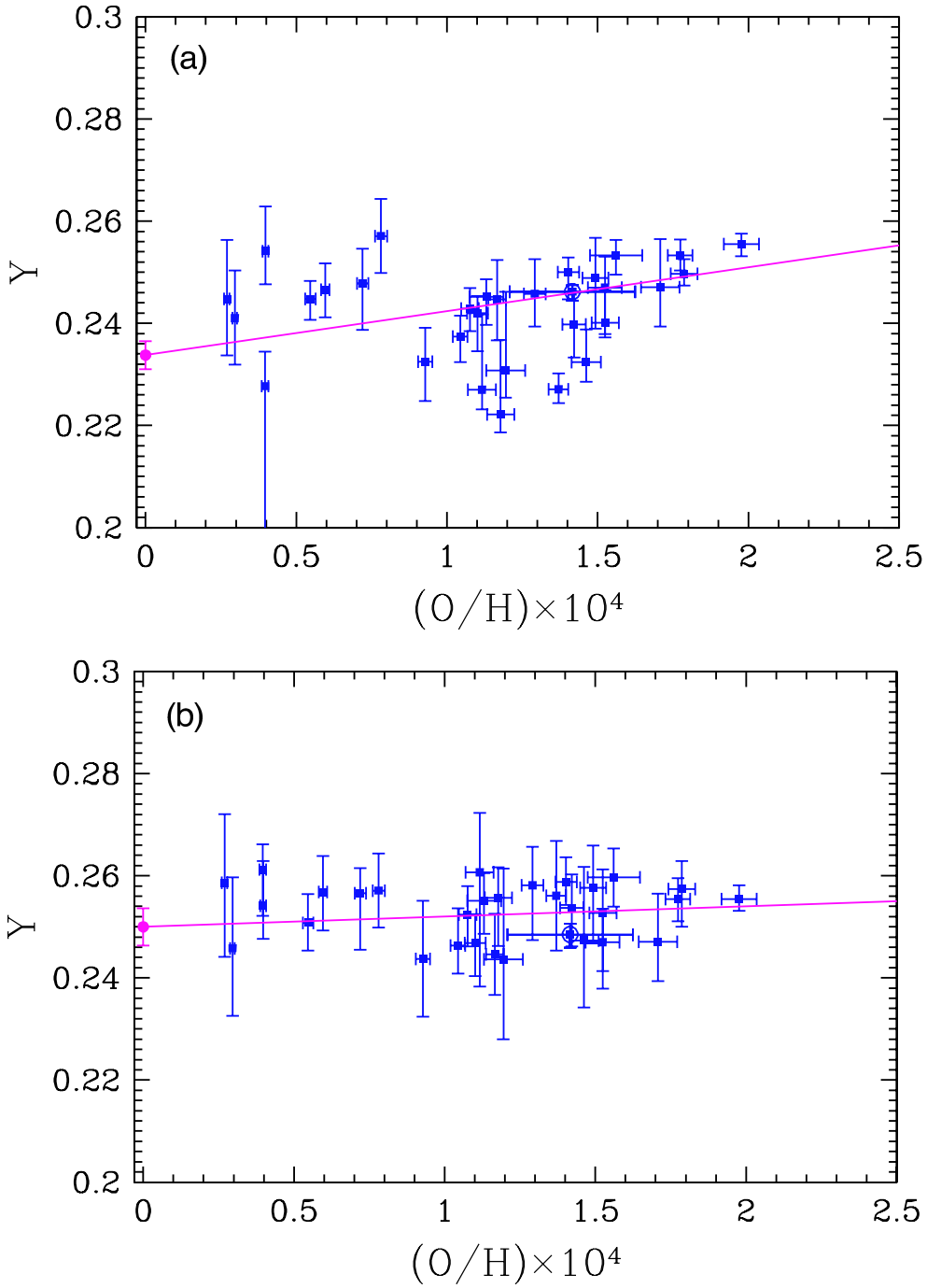

Fig. 1.— Helium mass fraction Y vs oxygen abundance O/H for 30 HII regions in IT04 (filled circle) and NGC346A (open circle) (a) without and (b) with steller absorption. The solid line represents the linear fit.

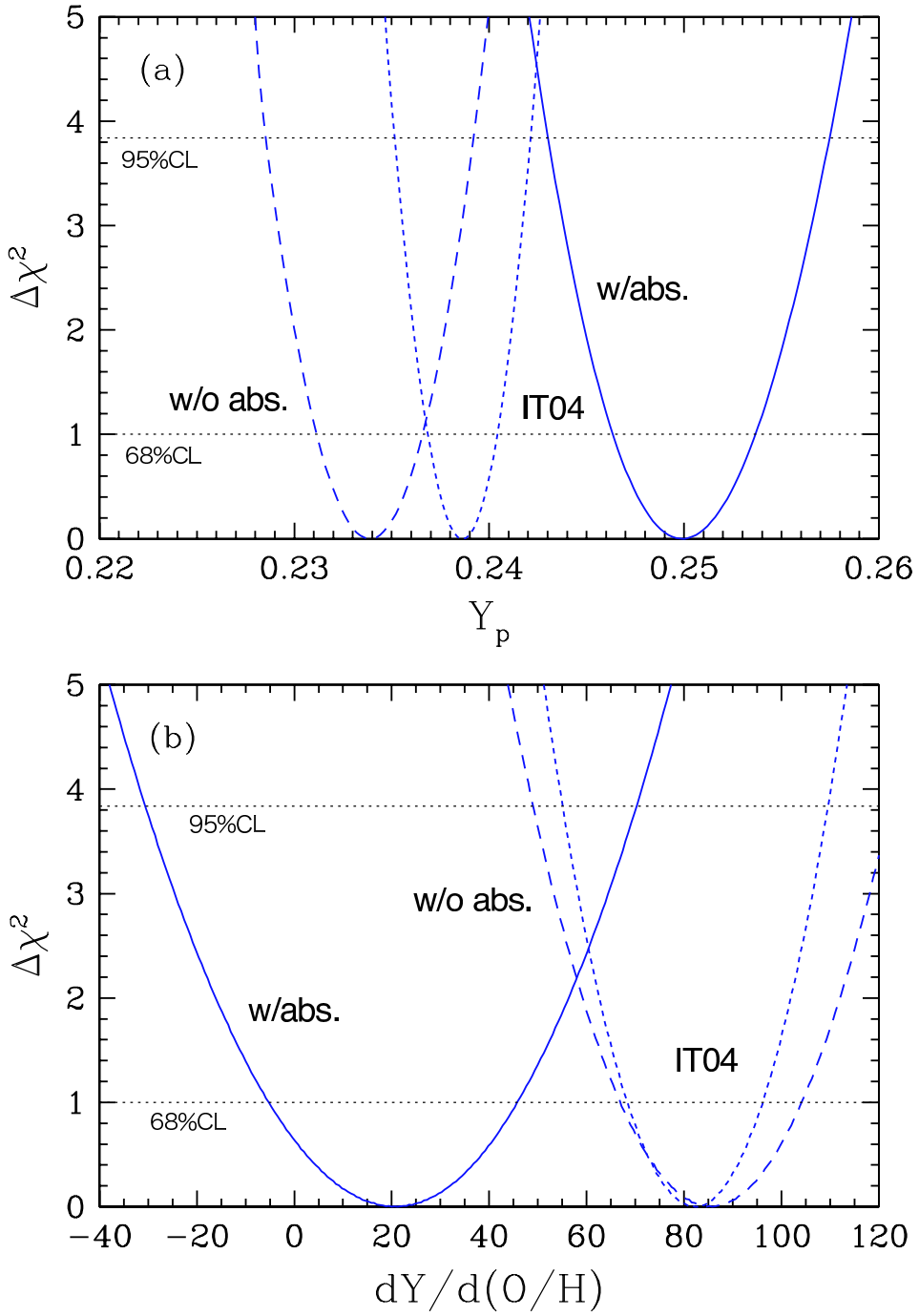

Fig. 2.— $\Delta\chi^2 = \chi^2 - \chi^2_{\rm min}$ for (a) Y_p and (b)dY/d(O/H). The solid and dashed curves denote the results with and without absorption, respectively. The dotted curve shows the helium abundances given in IT04. $\Delta\chi^2$ for 68% and 95% confidence levels are indicated.

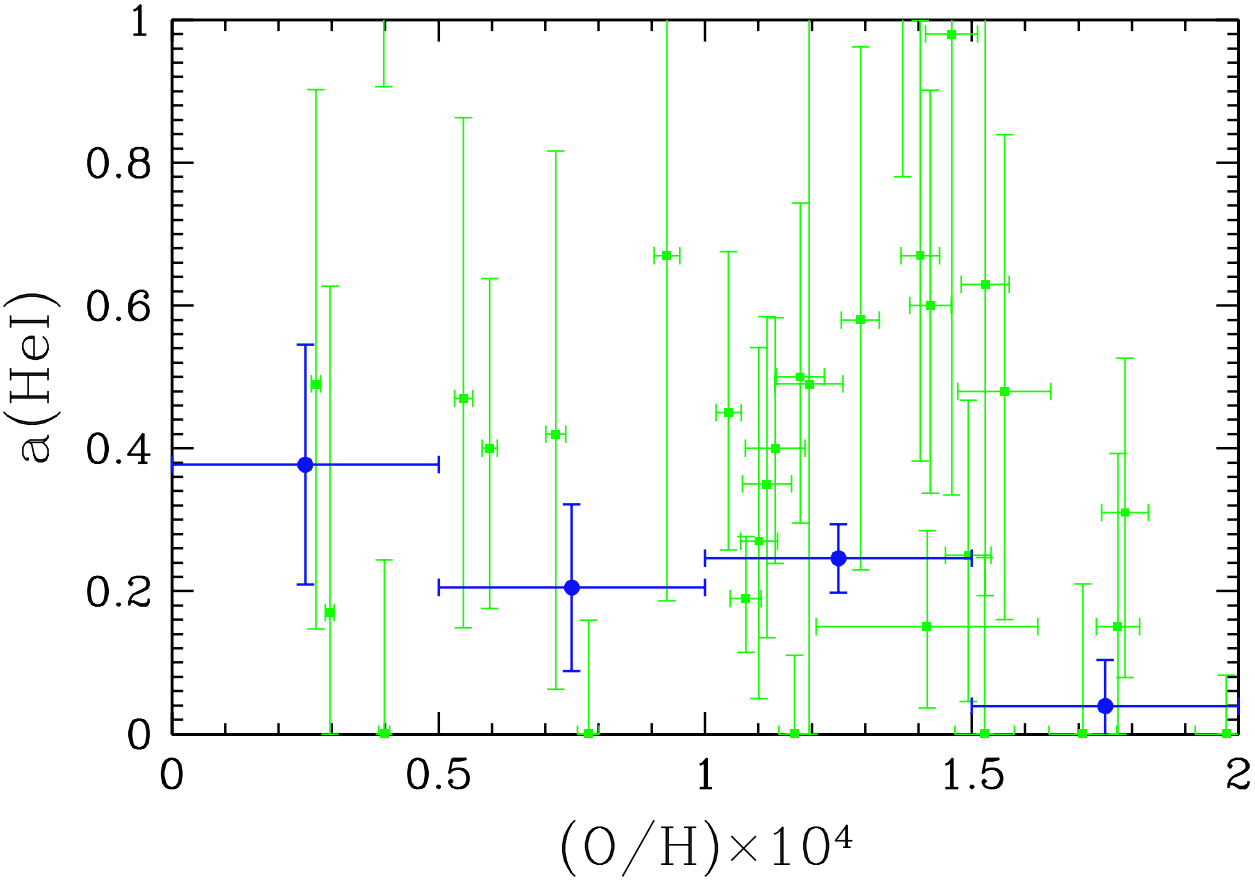

Fig. 3.— Stellar absorption for HeI emission lines vs the oxygen abundance (filled square). The binned average is shown by solid circles.